Surface & Coatings Technology 235 (2013) 10–14

Contents lists available at ScienceDirect

Surface & Coatings Technology

journal homepage: www.elsevier.com/locate/surfcoat

The electrochemical behavior of cobalt electrodeposits on 430 stainless steel as solid oxide fuel cell interconnect

Eric M. Garcia *

University of São João Del Rei Campus Sete Lagoas, Km 424-BR 040, Sete Lagoas, Minas Gerais 29800-000, Brazil

ARTICLE INFO

Article history:
Received 22 January 2013
Accepted in revised form 3 July 2013
Available online 10 July 2013

Keywords:
430 stainless steel
Cobalt electrodeposition
Interconnects
SOFC

ABSTRACT

In this paper, the electrochemical reactivity between $La_{0.6}Sr_{0.4}Co_{0.8}Fe_{0.2}O_3$ (LSCF) and cobalt-coated stainless steel was investigated in air at 700 °C. The cobalt electrodeposition onto ferritic stainless steel has an important role in decreasing of chromium poisoning on the cathode side of solid oxide fuel cells (SOFCs). The polarization resistance of a symmetrical cell composed by LSCF//YSZ//LSCF at 700 °C was evaluated using 430 stainless steel as electrical interconnects. The polarization resistance for cobalt-coated interconnects was 0.92 Ω cm^2 and for uncoated interconnects was 5.1 Ω cm^2. The formation of Co_3O_4 layer seems to block the chromium migration.

© 2013 The Authors. Published by Elsevier B.V. Open access under CC BY license.

1. Introduction

Metallic interconnects for solid oxide fuel cells (SOFCs) have attracted great attention in recent years. This is due to characteristics such as higher electronic and thermal conductivities, low cost and good manufacturability compared to traditional ceramic interconnects [1–5]. Many papers have been focused on ferritic stainless steel due its low cost and adequate linear thermal expansion coefficient ($11–12 \times 10^{-6}$ K^{-1}) [6,7]. However, under cathode working conditions (typically at 1123 K in air) the CrO_3 and $CrO_2(OH)_2$ evaporate from Cr_2O_3 [7] causing severe degradation (Eqs. (1) and (2)). Moreover the Cr(VI) can be reduced parallel with oxygen, reducing the lifetime of SOFCs [7,8].

$$1/2Cr_2O_{3(s)} + 3/4O_{2(g)} \rightarrow CrO_{3(g)} \quad (1)$$

tadata, citation and similar papers at core.ac.uk

brought to you by CORE

provided by Elsevier - Publisher Connector

The interaction between metallic interconnect and cathodes as LSCF ($La_xSr_{(1-x)}Co_yFe_{(1-y)}O_3$) has been investigated [9]. In literature it is related to the formation of $SrCr_2O_4$ at LSCF/ferritic stainless steel interface [10]. The reaction to form non-conductive $SrCr_2O_4$ could occur between gaseous CrO_3 and a nucleation agent, namely SrO segregated on the surface of LSCF electrodes, to form Cr–Sr–O nuclei [10]. $SrCr_2O_4$ is non-conductive and its formation leads to reduction of conductivity and porosity of cathode [10,11]. The deposition of reaction products showed in Eq. (3) was predicted to inhibit the cathodic oxygen reduction reaction at the three-phase boundary (TPB). To improve the surface electrical properties and reduce the amount of chromium in oxide layer, the semiconductor oxide coating has been proposed [12,13]. Cobalt oxide Co_3O_4 is a promising candidate because of its interesting conductivity (6.70 S cm^{-1}) and its adequate linear thermal expansion coefficient [14]. A good strategy to obtain the Co_3O_4 layer onto stainless steel is cobalt electrodeposition with subsequent oxidation in air at high temperatures [14].

In this paper, the 430 stainless steel surface was coated with cobalt by electrodeposition method followed by heat treatment at 700 °C for 45 h in air atmosphere. The effect of cobalt protection on there is a trend to reduce the operating temperature of SOFC. A temperature range of 400–600 °C is already envisioned by the researchers [13,14]. Thus the temperature used in this paper was 700 °C.

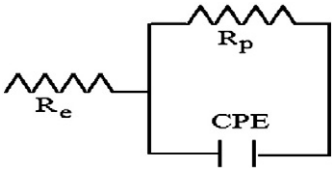

Fig. 1. Equivalent circuit between the LSCF cathode and YSZ electrolyte.

* Tel.: +55 31 3409 5714; fax: +55 31 3409 5700.
E-mail address: ericmgmg@hotmail.com.

0257-8972 © 2013 The Authors. Published by Elsevier B.V. Open access under CC BY license.
http://dx.doi.org/10.1016/j.surfcoat.2013.07.007

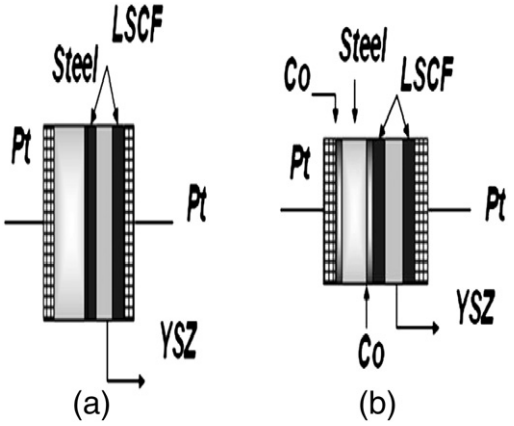

Fig. 2. (a) Cell Pt/LSCF//YSZ//LSCF/steel/Pt where the LSCF is in direct contact with metallic interconnect (430 stainless steel). (b) Cell Pt/LSCF//YSZ//LSCF/Co/steel/Co/Pt.

2. Experimental

2.1. Preparation of electrodeposition solutions

Cobalt was deposited by electroplating onto polished AISI 430 stainless steel substrates which had an area of 200 mm^2. The counter electrode was made of platinum, with area equal to 3.75 cm^2 and the reference electrode was saturated with Ag/AgCl/KCl. The electroplating bath was operated under the conditions of agitation at pH 3.0, current density of 100 mA cm^{-2}, temperature of 30 °C and charge density of 10.0 C cm^{-2}. The solution consisted of 300 g cobalt sulphate (MERCK) and 30 g of boric acid (MERCK) dissolved in 1 L of distilled water. The electrodeposited cobalt was analyzed by scanning electron microscopy and its thickness was approximately 1 μm.

2.2. Electrochemical measurements and material characterization

Electrochemical measurements were held with an AUTOLAB PGSTAT 302 with impedance module, FRA and GPES software. The electrochemical impedance spectroscopy measurements were performed in a frequency scale of 1.00×10^5 to 1.00×10^{-3} Hz with a signal amplitude of 10.0 mV. When a sinusoidal potential excitation (Eq. (3)) is applied to the electrode/solution interface, it causes an out of phase current response with respect to the applied sinusoidal potential (Eq. (4)) [1].

$$E_{(t)} = E_0 \sin(wt) \tag{3}$$

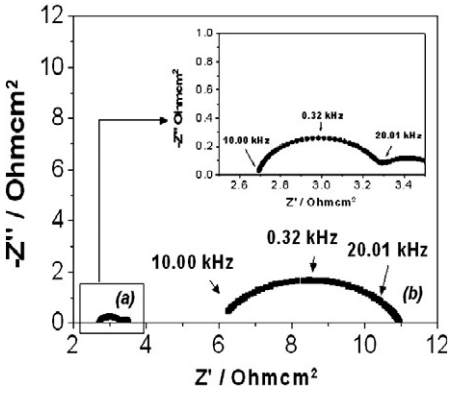

Fig. 3. Electrochemical impedance after 2 h in air at 700 °C for half-cell (a) Pt/LSCF//YSZ//LSCF/Co/steel/Co/Pt and (b) Pt/LSCF//YSZ//LSCF/steel/Pt.

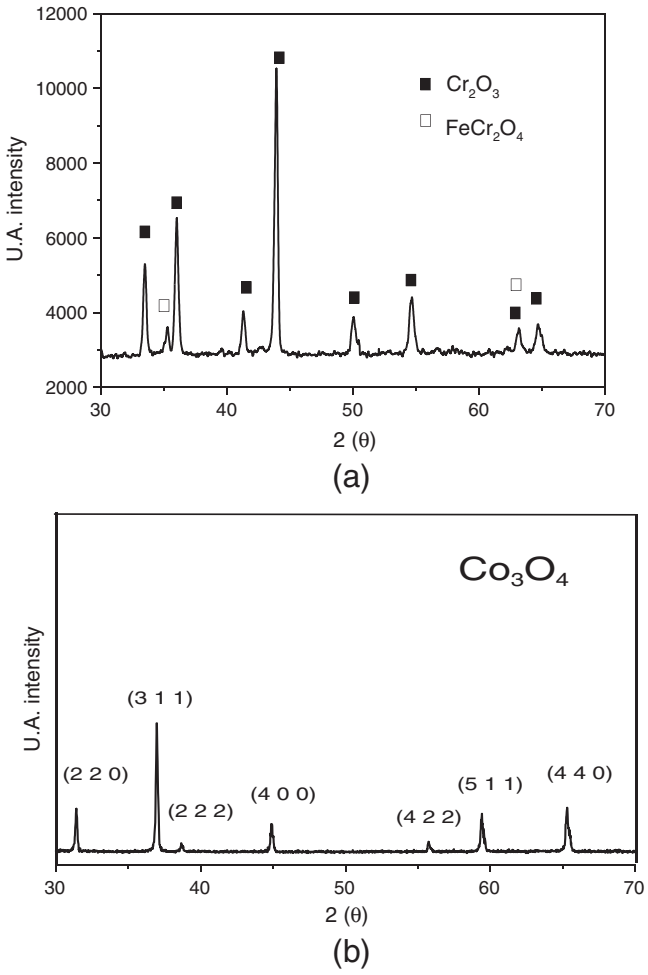

Fig. 4. The X-ray diffraction patterns of 430 stainless steel without (a) and with (b) cobalt after 45 h at 700 °C.

$$I_{(t)} = I_0 \sin(wt + \varphi) \tag{4}$$

Using Euler's formula, the electrochemical impedance, Z (w), can be expressed as a real part, Z′ (w), and an imaginary part, Z″ (w), (Eq. (5)):

$$Z_{(w)} = \frac{I_0 \sin(wt + \varphi)}{E_0 \sin(wt)} = Z'_{(w)} + iZ''_{(w)}. \tag{5}$$

In a system with a low contribution of mass transfer, the impedance can be predicted as the mathematical model shown in Eq. (6) [1].

$$Z_{(w)} = R_s + \frac{R_p}{1 - C^2 R_p{}^2 w^2} + \left[\frac{wCR_p{}^2}{1 - w^2 C^2 R_p{}^2}\right] \tag{6}$$

The mathematical model shown in Eq. (6) is equivalent to the circuit shown in Fig. 1. This figure represents the electrical interface LSCF/YSZ. In this circuit, R_e represents the electrolyte resistance, R_p represents the polarization resistance and CPE is the non-ideal capacitance of the electrical interface.

A steel plate was coated with cobalt and another plate was uncoated. These plates were subjected to a temperature of 700 °C for 45 h. The cross section of samples was analyzed by scanning electron microscopy (SEM). X-ray diffraction and energy dispersive X-ray of samples with and without cobalt were performed. The cobalt

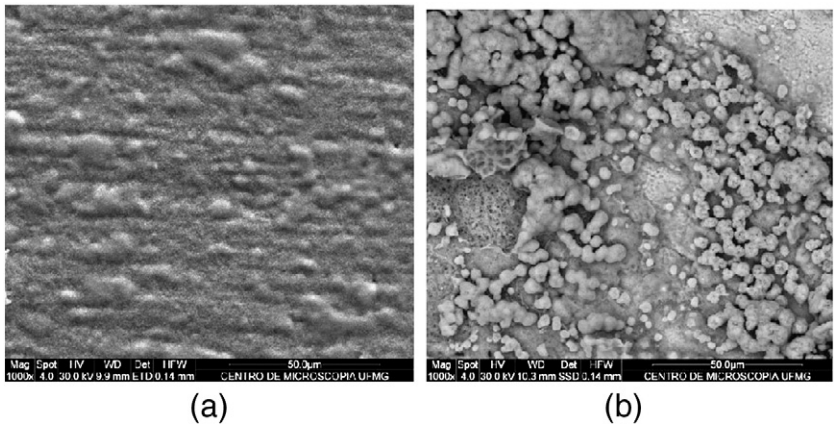

Fig. 5. The scanning electron microscopy (SEM) of 430 stainless steel with (a) and without (b) cobalt after 45 h at 700 °C.

electrodeposit characterization was performed in a JEOL JXA model 8900 RL.

3. Results and discussion

To investigate the effect of Cr poisoning on LSCF, the electrical polarization resistance was measured in air using the electrochemical impedance spectroscopy (EIS) at 700 °C. The reactivity study was performed on 430 stainless steel interconnects. The electrochemical interfaces of interest are shown in Fig. 2. In Fig. 2a, the LSCF is in contact with stainless steel. On the other hand, in Fig. 2b the LSCF is in contact with cobalt-coated stainless steel. The EIS diagrams after 2 h for cell Pt/LSCF//YSZ//LSCF/steel/Pt (where the interconnect is stainless steel) and Pt/LSCF//YSZ//LSCF/Co/steel/Co/Pt (where the interconnect is cobalt-coated stainless steel) are shown in Fig. 3a and b respectively. Comparing the two cases qualitatively, in the cell where interconnect was coated with cobalt, the polarization resistance was significantly smaller than uncoated interconnect. The polarization resistance for cell (a) was 0.92 Ω cm^2 (coated interconnect) and for cell (b) (uncoated interconnect) was 5.1 Ω cm^2. It must be taken into account that, in both cases, what was measured is the polarization resistance (R_p), in other words, the resistance for electron transfer through double-layer to promote the oxygen reduction ($O_2 + 2e^- \rightarrow 1/2\ O^{-2}$). The R_p is inevitably affected by area specific resistance (ASR) of interconnects (its limit value for SOFC applications is 0.10 Ω cm^2). Despite ASR not being taken into consideration in this paper, in our previous paper discussed only this aspect [10].

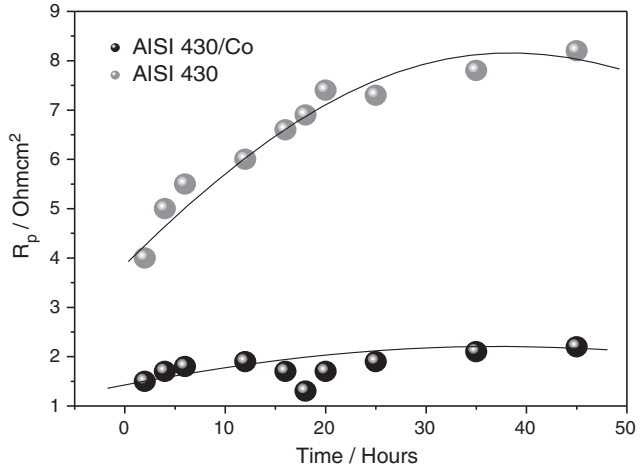

Fig. 6. The polarization resistance for half-cells Pt/LSCF//YSZ//LSCF/steel/Pt and Pt/LSCF//YSZ//LSCF/Co/steel/Co/Pt in air at 700 °C.

Fig. 4 shows the X-ray diffraction (XRD) patterns of 430 stainless steel/Co and 430 stainless steel after heat treatment at 700 °C for 45 h. When the cobalt is subjected to heating at 700 °C, a layer of Co_3O_4 is formed (Eq. (7)) [11].

$$3Co_{(s)} + 2O_{2(g)} \xrightarrow{800^\circ C} Co_3O_{4(s)} \quad (7)$$

However, in the steel without cobalt, the Cr_2O_3 is predominant, although the presence of $FeCr_2O_4$ can be also observed (Fig. 4a). The conductivity of Cr_2O_3 (0.003–0.05 S cm^{-1} at 800 °C [15,16]) is much lower than Co_3O_4 (6.7 S cm^{-1} at 1123 K in air [11]). This explains the higher values for R_p found for steel without cobalt (Fig. 3).

Fig. 5 shows the scanning electron micrograph (SEM) of 430 steel with (a) and without (b) cobalt coating after oxidation in air atmosphere for 45 h at 700 °C. The steel samples without cobalt (Fig. 5b) show great porosity and oxide spallation. The surface steel degradation (Fig. 5) occurs due to the formation of volatile Cr^{VI} species (Eqs. (1) and (2)) [16]. Through SEM, it can be seen that the porosity and oxide spallation have been significantly reduced in the steel with cobalt (Fig. 5a). The cobalt coated sample shows a more regular morphology than the uncoated sample. In this case the Co_3O_4 coating serves as a barrier to decrease Cr_2O_3 in the surface of the samples.

Fig. 6 presents the polarization resistance for symmetric cells at 700 °C in air for 45 h. For the cell where the interconnect does not have a cobalt layer, the polarization resistance shows an increase in time. For the cell in which cobalt-coated stainless steel was used the polarization resistance is practically constant over the time. Fig. 7 represents the LSCF surface after oxidation test. In Fig. 7a the LSCF was in contact with cobalt-coated stainless steel and in Fig. 7b it was in contact with pure stainless steel. It can be clearly seen that, in the LSCF sample in contact with uncoated steel, the chrome presence is evident in accord with EDX measurements (Fig. 7b). However when the LSCF is in contact with the cobalt-coated interconnect, the chromium presence is not evidenced. In this case, the Co_3O_4 prevents the solid state reaction of Cr_2O_3 with chromium diffusion from the LSCF. A test of conductivity with two probe methods was performed on steel samples. The separation of the two probes was 1 cm and the force applied was 1 kg. The sample without cobalt has the resistivity of 0.58 Ω cm. This value is a very different theoretical value for a mixture of Cr_2O_3 and $FeCr_2O_4$ (1.3×10^3 Ω cm [16]). This result is more compatible with metallic resistance. It means that the oxide layer on top of steel is very porous and discontinuous or imperfect. On the other hand, in the steel with cobalt coating the resistivity obtained is 0.95×10^8 Ω cm. This value is very close to the resistivity

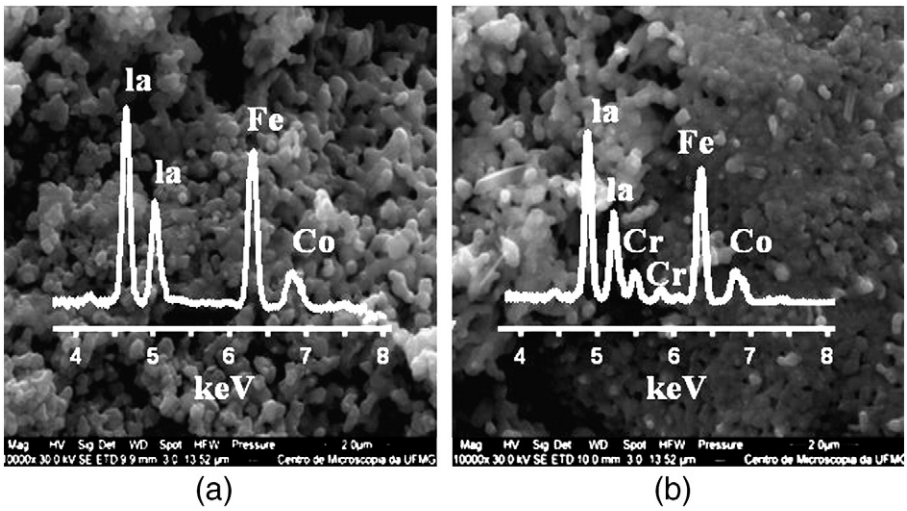

Fig. 7. The SEM and EDX for LSCF surface after the test. In (b) the LSCF was in contact with steel cobalt coated and in (c) without cobalt coating.

value of Co_3O_4 (1.01×10^8 Ω cm [12]). This shows that Co_3O_4 layer is much more compact and dense compared to 430 stainless steel. As it has been studied by our research group [11], when the steel is cobalt coated, the formation of Co_3O_4 layer inhibits the chromium oxide volatilization. On the other hand at the interface without cobalt the formation of Cr_2O_3 can lead to formation of insulating phases such as $SrCr_2O_4$.

To investigate the Cr distribution in detail, we conducted EDX point-scan analysis of sample cross-sections (Fig. 8). The cobalt content is higher than Cr content after interface. This can be indicative that Co_3O_4 serves as a barrier to decrease the Cr_2O_3 in the surface samples. When the steel is recovered by cobalt, the formation of Co_3O_4 layer inhibits the Cr_2O_3 formation [11].

4. Conclusion

Although the exposure time used in this paper was relatively short (45 h), the cobalt electrodeposition technique and subsequent oxidation treatment are effective methods to produce Co_3O_4 coatings on 430 stainless steel. The polarization resistance of LSCF in contact with cobalt coated steel is 0.92 Ω cm^2 and with uncoated steel was 5.1 Ω cm^2. The cell in which the steel was covered with cobalt shows a more regular morphology than the uncoated one; moreover, in this case the polarization resistance of LSCF increases almost linearly with time. In the cell in which cobalt coated steel was used, the polarization resistance is practically constant over time. In accord with EDX

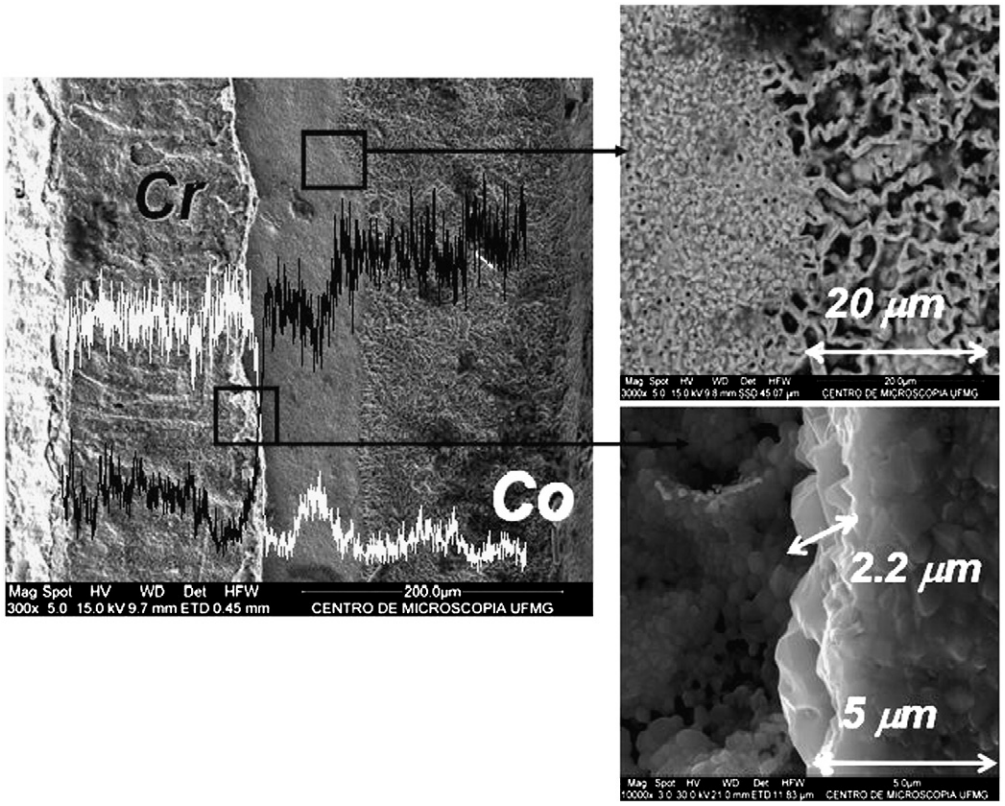

Fig. 8. SEM and EDX in the cross-section of 430 stainless steel with cobalt coating cobalt after 45 h at 700 °C.

measures, the formation of Co_3O_4 layer inhibits the chromium oxide volatilization.

Acknowledgments

The authors acknowledge the UFSJ and the CNPq for their financial support.

References

[1] S. Nakahara, S. Mahajan, J. Electrochem. Soc. 127 (1980) 283–286.
[2] M. Lang, T. Franco, G. Schiller, N. Wagner, J. Appl. Electrochem. 32 (2002) 871–879.
[3] P. Piccardo, P.E. Gannon, S. Chevalier, M. Viviani, A. Barbucci, Surf. Coat. Technol. 202 (2007) 1221–1225.
[4] J.W. Fergus Mater, Sci. Eng. 397 (2005) 271–280.
[5] S. Chevalier, G. Caboche, K. Przybylski, T. Brylewski, J. Appl. Electrochem. 39 (2009) 529–534.
[6] L. Repetto, P. Costamagna, J. Appl. Electrochem. 38 (2008) 1005–1010.
[7] V.I. Gorokhovsky, R. Bhattacharya, D.G. Bhat, Surf. Coat. Technol. 140 (2001) 82–87.
[8] Y. Liu, D.Y. Chen, Int. J. Hydrogen Energy 34 (2009) 9220–9226.
[9] A. Petric, H. Ling, J. Am. Ceram. Soc. 90 (2007) 1515–1520.
[10] E.M. Garcia, H.A. Tarôco, T. Matencio, R.Z. Domingues, J.A.F. dos Santos, M.B.J.G. Freitas, J. Appl. Electrochem. 41 (2011) 1373–1378.
[11] E.M. Garcia, H.A. Taroco, T. Matencio, R.Z. Domingues, J.A.F. dos Santos Int, J. Hydrogen Energy 37 (2012) 6400–6410.
[12] M.B.J.G. Freitas, E.M. Garcia, Celante J. Appl. Electrochem. 39 (2009) 601.
[13] K.T. Lee, C.M. Gore, E.D. Wachsman, J. Mater. Chem. 22 (2012) 22405–22408.
[14] C. Xia, M. Liu Solid, Solid State Ionics 144 (2001) 249–255.
[15] E.M. Garcia, J.S. Santos, E.C. Pereira, M.B.J.G. Freitas, J. Power Sources 185 (2008) 549.
[16] W.Z. Zhu, S.C. Deevi, Mater. Sci. Eng., A 348 (2003) 227–243.